



Pharmacological inhibition of GRK2 improves cardiac metabolism and function in experimental heart failure

Michele Ciccarelli^{1*} , Daniela Sorriento² , Antonella Fiordelisi², Jessica Gambardella² , Antonietta Franco² , Carmine del Giudice² , Marina Sala³ , Maria Gaia Monti², Alessia Bertamino³, Pietro Campiglia³ , Marco Oliveti¹ , Paolo Poggio⁴ , Giovanna Trinchese⁵ , Gina Cavaliere⁵, Ersilia Cipolletta², Maria Pina Mollica⁵, Domenico Bonaduce⁶, Bruno Trimarco²  and Guido Iaccarino^{2*} 

¹Department of Medicine, Surgery, and Dentistry, University of Salerno, Baronissi, Italy; ²Department of Advanced Biomedical Sciences, 'Federico II' University of Naples, Naples, Italy; ³Department of Pharmacy, University of Salerno, Fisciano, Italy; ⁴Centro Cardiologico Monzino IRCCS, Milan, Italy; ⁵Department of Biology, 'Federico II' University of Naples, Naples, Italy; ⁶Department of Translational Medical Sciences, 'Federico II' University of Naples, Naples, Italy

Abstract

Aims The effects of GRK2 inhibition on myocardial metabolism in heart failure (HF) are uncharted. In this work, we evaluated the impact of pharmacological inhibition of GRK2 by a cyclic peptide, C7, on metabolic, biochemical, and functional phenotypes in experimental HF.

Methods and results C7 was initially tested on adult mice ventricular myocyte from wild type and GRK2 myocardial deficient mice (GRK2-cKO), to assess the selectivity on GRK2 inhibition. Then, chronic infusion of 2 mg/kg/day of C7 was performed in HF mice with cryogenic myocardial infarction. Cardiac function *in vivo* was assessed by echocardiography and cardiac catheterization. Histological, biochemical, and metabolic studies were performed on heart samples at time points. C7 induces a significant increase of contractility in wild type but not in adult ventricle myocytes from GRK2-cKO mice, thus confirming C7 selectivity for GRK2. In HF mice, 4 weeks of treatment with C7 improved metabolic features, including mitochondrial organization and function, and restored the biochemical and contractile responses.

Conclusions GRK2 is a critical molecule in the physiological regulation of cardiac metabolism. Its alterations in the failing heart can be pharmacologically targeted, leading to the correction of metabolic and functional abnormalities observed in HF.

Keywords Remodelling; Hypertrophy; Beta; Adrenergic; Metabolism; Mitochondria

Received: 25 November 2019; Revised: 27 March 2020; Accepted: 31 March 2020

*Correspondence to: Guido Iaccarino, MD, PhD, FESC, Department of Advanced Biomedical Sciences, Federico II University, Via Pansini 5, Building 2, 80131 Napoli, Italy. Email: guiacar@unina.it

Michele Ciccarelli, MD, PhD, Department of Medicine, Surgery, and Dentistry, University of Salerno, Via S. Allende, 84081, Baronissi (SA), Italy. Tel: +39089672335. Email: mciccarelli@unisa.it

Introduction

Heart failure (HF) is a progressive syndrome that leads to the disability of the cardiac pump to warrant an efficient blood supply to the different organs and systems. This is a multifaceted condition that represents the leading cause of disability and mortality around the world. Researchers seek new treatments that can help to tailor therapy for different patients, and the quest is actively ongoing. The clinical variability mirrors a biochemical complexity, and the alterations of several signalling are the most critical targets for an effective

amelioration of prognosis in patients with HF. Indeed, the failing cardiomyocyte is not only less responsive to the adrenergic stimulation, but it is also out of energy, with mitochondrial dysfunction leading to the impaired use of metabolic substrates for production of ATP,¹ increased ROS production, and altered calcium handling.^{2–4} These hallmarks of HF involve alterations and participation of specific molecules that can be potentially targeted through pharmacological approaches, narrowing the molecular target to those proteins that have demonstrated to be at the same time functionally, biochemically, and energetically relevant.³ This is the case for

the G protein-coupled receptor kinase 2 (GRK2), whose molecular complexity and mechanistic implications in HF are well demonstrated and documented.^{5,6} Indeed, the increased levels of GRK2 during chronic HF promote the desensitization and down-regulation of the β adrenergic receptor (β AR), induce cardiac insulin resistance, and reduce cardiac metabolic plasticity.⁷ In particular, alterations of cardiac metabolism are an early marker of HF that anticipates the systolic dysfunction and ventricle remodelling.⁷

Furthermore, GRK2 localizes at mitochondria⁸ where it seems, in the long run, to promote a pro-death signal pathway.⁹ Although previous literature shows the possibility to restore cardiac contractility by targeting GRK2 with different strategies, so far, no information is available as to the effects of GRK2 inhibition on cardiac metabolism and mitochondrial function in the failing heart. Targeting GRK2 has been earlier obtained by overexpression of carboxyl portion of GRK2 (also termed β ARKct), a construct that interferes with GRK2 localization at the plasma membrane, with benefits on cardiac function in HF models in mice.^{10,11} However, β ARKct specificity to inhibit GRK2 has been questioned because this molecule also blocks β Arrestins and $\beta\gamma$ dependent signalling. β ARKct also failed to deliver to the clinical scenario due to its size (\approx 200 amino acids) and its need for gene delivery tools to be expressed in target tissues. Screening libraries of pharmacological compounds^{12,13} lead to the discovery that paroxetine is an effective GRK2 inhibitor.¹⁴ Nevertheless, the need to be used in relatively high doses¹⁵ and possibly elevating the risk of neurological complications has limited its use. Another class of heterocyclic compounds was developed by Takeda Pharmaceutical Company Ltd. that exhibited high selectivity for GRK2 but never tested in the setting of HF.¹⁶

Recently, we have provided evidence that short peptides derived from HJ loop of GRK2^{17,18} are potent inhibitors of GRK2 and possess favourable metabolic effects in animal models of Type 2 diabetes¹⁹ and insulin resistance.²⁰ In the present study, we evaluated the effects of systemic administration of an HJ based cyclic peptide 'C7' on the cardiac metabolism and mitochondrial abnormalities observed in a mouse model of HF post-myocardial infarction (post-MI HF).

Methods

GRK2 inhibitor

The GRK2 inhibitor 'C7' and its inhibitory biochemical properties were previously described.¹⁷ The peptide is solubilized in water to the final concentrations indicated. We evaluated (i) C7 selectivity and contractile response on cardiomyocytes isolated from transgenic mice with cardiac-specific knockout of GRK2 gene (MHCcre GRK2fl/fl; GRK2-cKO)²⁰ and GRK2 fl/fl (control); (ii) titration of C7 in healthy animals; (iii) effects of GRK2 inhibition by C7 in an animal model of post-MI HF.

Experimental animals

C57BL/6, MHCcre GRK2fl/fl, and GRK2fl/fl male mice (Jackson Laboratories, USA) weighing 25 ± 0.5 g, 12 weeks old, with conventional microbiological status, were used. Animals were kept in a controlled environment (12:12 h light/dark period; 23°C; 55–60% humidity; and free access to water and chow). Transgenic MHCcre GRK2fl/fl and GRK2fl/fl mice were obtained as follows: mice with cardiac overexpression of CRE recombinase (α MHC-Cre, Jackson Laboratories) were bred with mice bearing GRK2 gene flanked by p-lox sequences (GRK2 fl/fl) to generate cardiac GRK2-deleted mice (GRK2-cKO), initiated by the activation of the α MHC-promoter. Genotyping of the animal was performed as previously described.²¹

Animals were acclimatized for at least 7 days before the experiments and surgery, which were approved and conducted in accordance with the *Guide for the Care and Use of Laboratory Animals* published by the US National Institutes of Health (NIH Publication No. 85-23, revised 1985) and approved by the Italian Ministry of Health—DG on animal's wellness and veterinary drugs (#674/2015-PR). Animal studies are reported in compliance with the ARRIVE guidelines.^{22,23}

Evaluation of C7 selectivity and contractile response on cardiomyocytes isolated from mice

Adult mice ventricular myocytes (AMVMs) were then isolated from $n = 4$, GRK2 fl/fl and MHCcre GRK2 fl/fl 12-week-old mouse hearts by a standard enzymatic digestion procedure using Langerdhoff system as described.⁷ Myocyte contractility was evaluated after stimulation with the vehicle, isoproterenol (iso, 1 μ M), C7 (1 μ M), and C7 plus iso, as described in detail in the Supporting Information.

Evaluation of GRK2 inhibition by C7 in healthy animals

C57/Bl6 mice of the age of 12 weeks were randomly subjected to intraperitoneal (ip) injection of C7 at the dose of 2 mg/kg/100 μ L or 4 mg/kg/100 μ L ($n = 6$ per group) with or without ip injection of iso (10 ng). Cardiac dimensions and ejection fraction (EF) were evaluated in by cardiac ultrasounds (CUS) (Vevo 2100, Visualsonic) before injection and at 10', 30', 60', and 90'. In another set of experiments, heart samples were collected at basal and 30' post injection to measure cAMP production ($n = 4$ per group) as detailed in the Supporting Information.

Evaluation of GRK2 inhibition by C7 in the animal model of heart failure post-myocardial infarction

We used male C57/Bl6 mice at the age of 12 weeks. MI was induced as described previously using a model of cryo-infarction that produces a highly reproducible loss of myocardium.^{24,25} Adult male (25–30 g) mice were anaesthetised using a 2% isoflurane (v/v) oxygen mixture, and after ensured the absence of movement, flexor, and pedal reflex, the heart was exposed as previously described.²⁶ Correctly, the fourth intercostal space was exposed, and a small hole was made with a mosquito clamp to open the pleural membrane and pericardium. With the clamp slightly open, the heart was smoothly and gently ‘popped out’ through the hole. Cryothermia was then applied to left ventricle anterior wall by use of a 6 mm² cryoprobe for 15 s, leading to a highly reproducible myocardial damage²⁴ of the left ventricle anterior wall (Supporting Information, *Figure S1A*). Sham animals were subjected to heart exposure without cryo-injury. At 6 weeks after surgery, HF was confirmed by CUS, based on reduced EF (<50%) and increased LVEDd (>4.5 mm). HF mice were randomized to different treatment and through subcutaneous implantation of a micro-osmotic pump (Alzet, mod 1004) received C7, 2 mg/kg/day or vehicle for 4 weeks ($n = 12$ per group). The dose of 2 mg/kg/day was defined according to the results in healthy mice. At the end of the treatment, mice were subjected to echocardiography and terminal haemodynamic. Heart samples were then collected for biochemical, metabolic, and histological assessment. Histological measurements and quantification were performed by three blinded investigators, to avoid any source of bias, as described in the legends. A complete description of methodologies is in the Supporting Information.

Statistical analysis

The results are expressed as mean \pm SEM of independent experiments as indicated in figure legends. We used Prism 7 (GraphPad, USA) and SPSS 24 (IBM, USA) to perform statistical analysis using a *t*-test, one-way and two-way ANOVA for comparisons among different time points or dosages and between experimental groups, as appropriate. $P < 0.05$ was considered significant. When ANOVA demonstrated a significant effect, a Bonferroni *post hoc* test was performed.

Results

Effects of GRK2 inhibition on isolated ventricular cardiomyocyte and in mice

To evaluate the specificity of the effects of C7 on cardiac cell contractility, we tested it on isolated AMVM from GRK2-cKO

and control mice. It is known that GRK2 regulates β AR signaling through the mechanism of desensitization and down-regulation. β AR stimulation with ISO induces a rapid increase of FS% in both control and GRK2-cKO AMVM. FS is significantly higher in AMVMs from GRK2-cKO because of GRK2 gene removal (*Figure 1A*). C7, similarly to ISO, prompts cardiac cell contractility and significant increases FS% in AMVM from control but not GRK2-cKO mice (*Figure 1A*). The GRK2 inh enhances iso effect on cell shortening in control AMVM, which is not present in GRK2-cKO (*Figure 1A*). Therefore, we tested C7 in healthy mice to assess the physiological consequences of GRK2 inhibition. As evaluated by CUS, C7 acutely produces a significant increase in the heart rate at 10 min post ip injection, accompanied by a reduction of left ventricle diastolic diameter (*Figure 1EC–1*), in a dose-dependent manner (2 mg/kg/100 μ L and 4 mg/kg/100 μ L). These effects disappear within 90 min post injection (*Figure 1FC–1*) and heart rate, left ventricle diameter, and EF to basal levels (*Figure 1EC–1*). Iso, as expected, increases cardiac functions at 10 and 30 min post injection, returning at the resting condition within 90 min post injection. The injection of either doses of GRK2 inh (2 or 4 mg/kg) strongly enhance the effects of iso on the cardiac functions (*Figure 1C–1E*). The positive inotropic and chronotropic effects of the GRK2 inh are paralleled by increased systolic pressure and cAMP production (Supporting Information, *Figure S1B* and *S1C*).

Cardiac volume and function are improved by GRK2 inhibitor cyclic peptide in mice with heart failure post-myocardial infarction

Based on the pharmacological data collected in healthy mice, we evaluated the effects of C7 in mice with post-MI HF at the dose of 2 mg/kg/day (GRK2 inh). As shown in *Figure 2A* and *2B* and Supporting Information, *Table S1* and *Figure 1D*, MI of the left ventricle anterior wall induces in 6 weeks induces statistically significant left ventricle dilation with the deterioration of systolic cardiac function. At this time point, we started continuous delivery of the C7 or vehicle for 4 weeks by intraperitoneal implantation of osmotic mini-pumps. Higher HR at baseline characterizes post-MI HF with reduced chronotropic reserve after ISO (*Figure 2C*). C7 reduces resting HR and restores chronotropic reserve in response to ISO (*Figure 2C*). C7-treated but not sham-treated post-MI HF group shows a significant reduction of left ventricle dimension, amelioration of EF and of +dP/dT both at baseline and after stimulation with ISO (*Figure 2A*, *2B*, and *2D*).

Similarly, post-MI HF group shows an altered diastolic function. Indeed, cardiac haemodynamic displays a blunted $-dP/dT$ in HF group respect to sham. C7 substantially ameliorates left ventricle pressure variation after ISO in post-MI HF

Figure 1 The acute effects of GRK2 inh on isolated AMVM and in healthy mice. (A) FS (%) in AMVM challenged with the vehicle, iso (1 μ M), GRK2 inh (1 μ M), or both ($n = 3$ independent experiments). Iso produces a significant increase in FS% in both AMVMs from GRK2 fl/fl and MHCcre GRK2 fl/fl ($^*P < 0.05$ vs. vehicle) but more pronounced in MHCcre GRK2 fl/fl ($^{**}P < 0.05$ vs. GRK2 fl/fl). GRK2 inh induces a significant increase of FS% in AMVMs from GRK2 fl/fl ($^!P < 0.05$ vs. vehicle) and enhances iso effect on cell shortening ($^!P < 0.05$ vs. iso alone). GRK2 inh does not exert any effects on cell shortening in MHCcre GRK2 fl/fl. AMVM, adult mice ventricular myocyte; FS, fractional shortening; Iso, isoproterenol; GRK2 inh, G protein-coupled receptor kinase 2 inhibitor. (B–D) Mice subjected to a single ip injection of C7 (2 or 4 mg/kg/100 μ L) with or without iso ($n = 5$ independent experiments). Cardiac functions evaluated by Ultrasound. GRK2 inhibition (2 and 4 mg/kg/100 μ L) significantly increases heart rate, systolic function, and reduces LVDd at 10' and 30' with the return to baseline at 90' post injection ($^{**}P < 0.05$ vs. vehicle). Iso increases cardiac function ($^!P < 0.05$ vs. vehicle). GRK2 inhibition (2 and 4 mg/kg/100 μ L) enhances iso effects on cardiac functions ($^!,^{!}P < 0.05$ vs. iso).

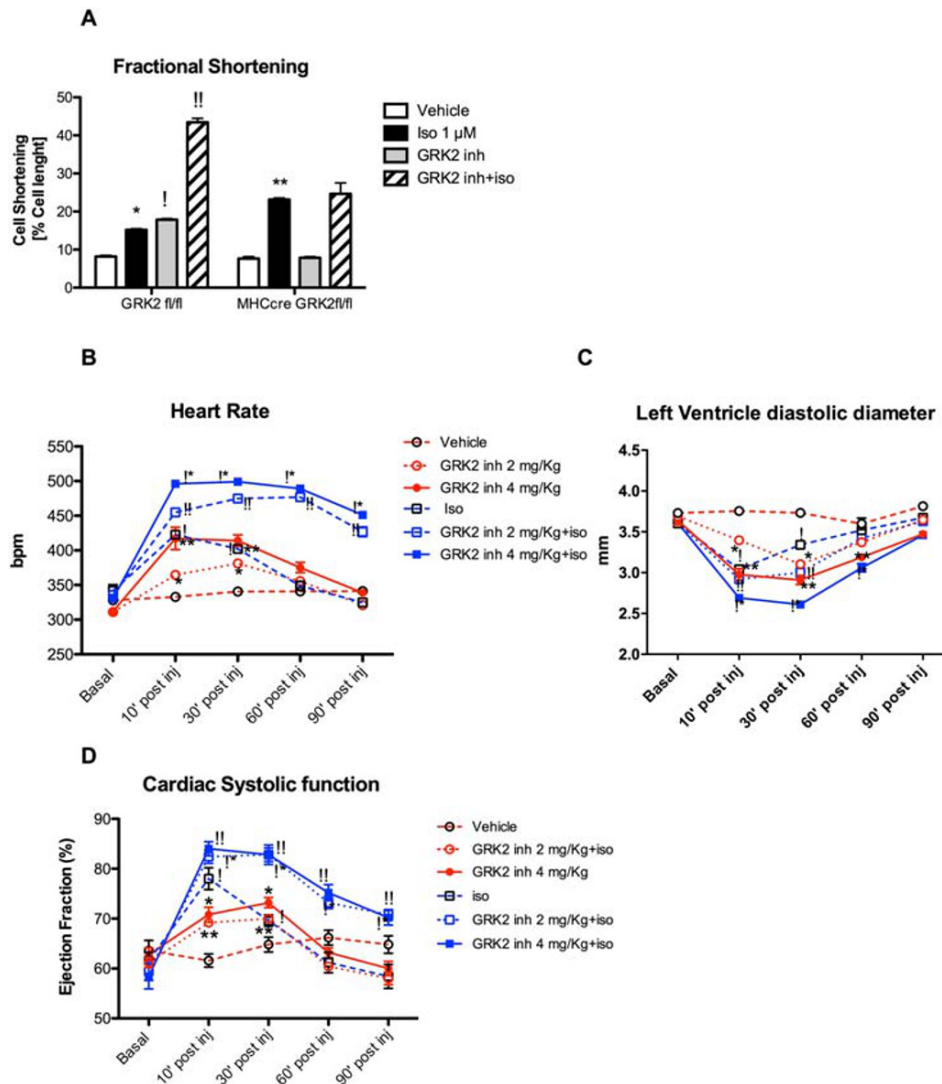


(Figure 2E). Accordingly, GRK2 inhibition with C7 reduced LV end-diastolic pressure (Figure 2F).

Effects of GRK2 inhibitor cyclic peptide on cardiac geometry, histology in failing hearts

Post-MI HF mice show eccentric cardiac hypertrophy (Figure 3CA–3). C7 treatment reduces the cardiac size (Figure 3A and 3B) and corrects RWT (Figure 3C). The results are

confirmed by measurements of cardiac myocyte transverse sections (Figure 3D and 3E), showing that the C7 counteracted MI-induced increase of myocyte cross-sectional area.

We then evaluated the effects of the chronic administration of the peptide on cardiac collagen deposition by Masson trichrome staining (Supporting Information, Figure S1E; Figure 3F and 3G). C7 markedly reverses the extensive collagen deposition observed in sham-treated post-MI HF animals.

Figure 2 Reduced cardiac dilation and improved function in post-MI HF mice treated with GRK2 inhibitor. (A, B) Left ventricle diastolic diameter (LVDD) and EF measured by serial echocardiography ($n = 12$ per group). Induced MI led to a progressive increase of LVDD and reduced EF, becoming significant at 6 weeks post surgery (* vs. sham, $P < 0.05$). GRK2 inhibitor treatment arrests cardiac dilation and promotes amelioration of systolic cardiac function in HF ($^!$ vs. post-MI HF, $P < 0.05$). (c-f) Functional response to acute iso infusion in vivo, illustrating heart rate, and $\pm dp/dt$ max response to graded concentrations of the catecholamine ($n = 6$, per group). HR is higher in post-MI HF mice respect to sham at baseline (* vs. sham, $P < 0.05$). No significant differences are evident between sham and HF groups treated with GRK2 inh at 2 mg/kg/day. $\pm dp/dt$ values are reduced upon iso iv infusion with depressed diastolic function and increased left ventricle diastolic pressure in post-MI HF ($^!$ vs. sham, $P < 0.05$). GRK2 inhibitor treatment improved cardiac contractility in mice with HF along with improved diastolic function and reduced left ventricle pressure ($^!$ vs. post-MI HF). EF, ejection fraction; HF, heart failure; Iso, isoproterenol; LVDD, left ventricle diastolic diameter; MI, myocardial infarction; other abbreviations as in previous figures.

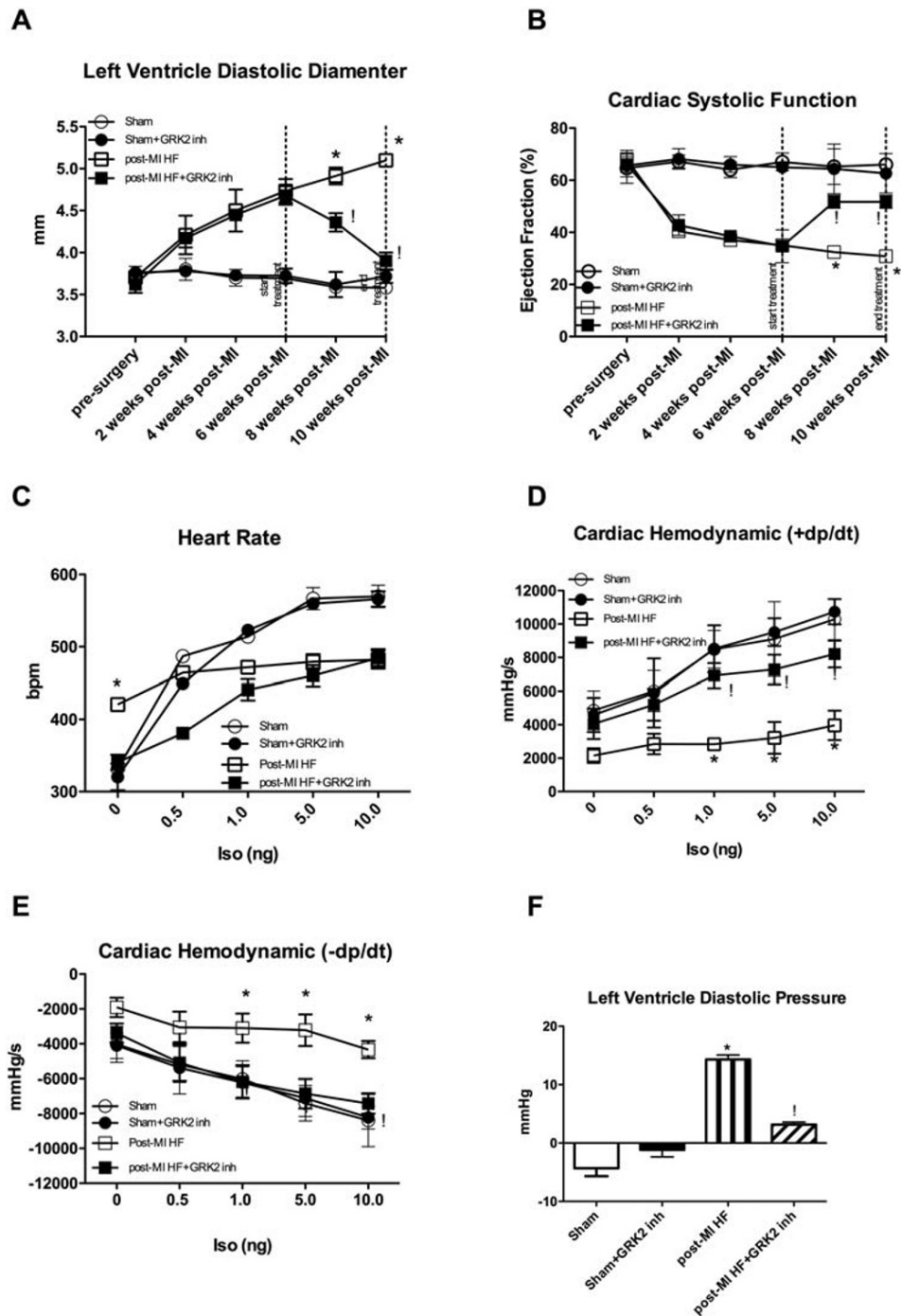


Figure 3 Reverse cardiac remodelling induced by the GRK2 inhibitor. (A–C) Cardiac Hypertrophy, left ventricle mass (LVm) corrected by tibia length and RWT were evaluated by HW/BW ratio and echocardiography ($n = 12$ per group). HW/BW and LVm increase in post-MI HF treated with vehicle (* vs. sham, $P < 0.05$) with a significant reduction in the group treated with the GRK2 inhibitor 2 mg/kg/day ($^!$ vs. post-MI HF, $P < 0.05$). RWT decreases in HF group (* vs. sham, $P < 0.05$) and normalized by treatment ($^!$ vs. post-MI HF, $P < 0.05$). (D, E) Fluorescence-tagged wheat germ agglutinin ($n = 4$ per group) shows increased cardiac myocyte cross-sectional area in post-MI HF mice (* vs. sham, $P < 0.05$; magnification 9200, scale bar = 15 μm) with significant reduction with GRK2 inhibitor treatment ($^!$ vs. post-MI HF, $P < 0.05$). Quantification was performed by three blinded investigators (D. S., A. F., and C. D. G.). (F, G) Masson's trichrome staining ($n = 4$ per group; magnification 9300, scale bar = 15 μm) also revealed an increase in interstitial fibrosis, quantified as described in Methods, in post-MI HF group (* vs. sham, $P < 0.05$; $n = 3$ per group) with a significant reduction induced by GRK2 inhibitor treatment ($^!$ vs. post-MI HF, $P < 0.05$). Quantification was performed by three blinded investigators (D. S., A. F., and C. D. G.). HW/BW, heart weight/body weight; LVm, left ventricle mass; RWT, relative wall thickness; other abbreviations as in previous figures.

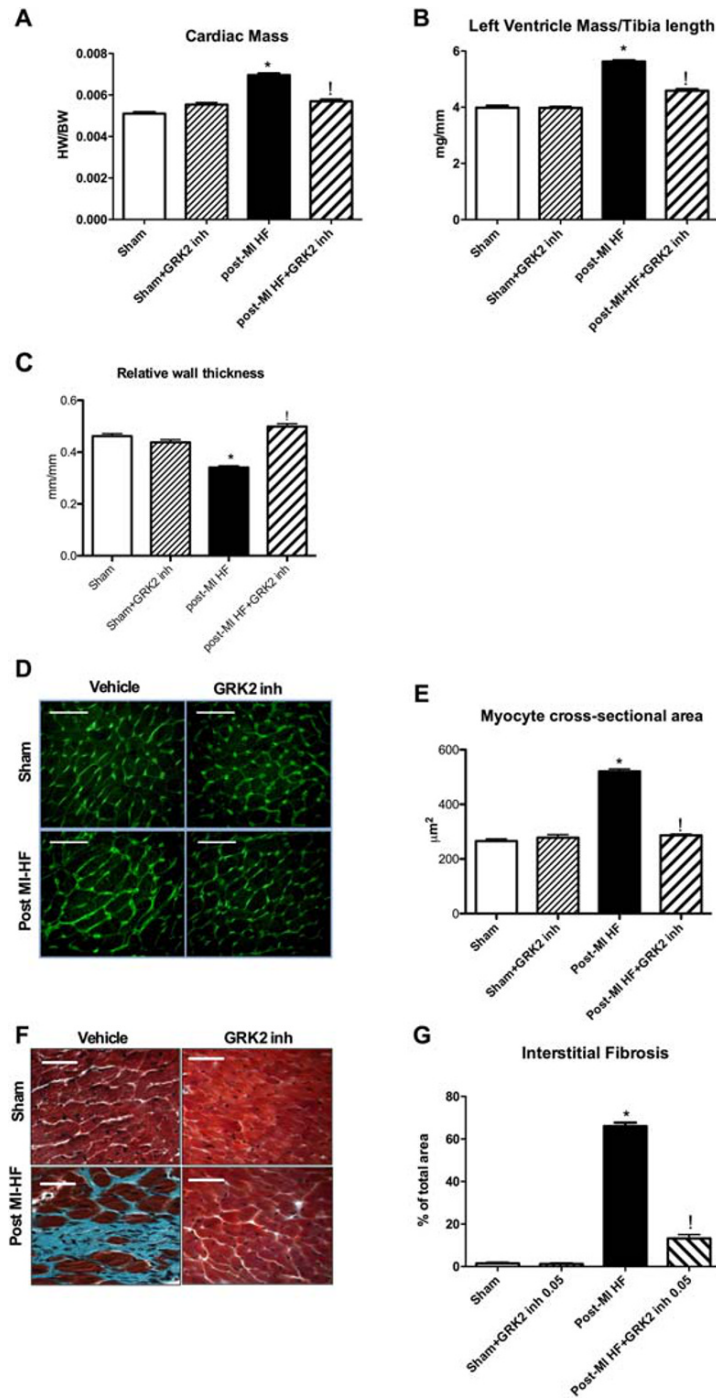
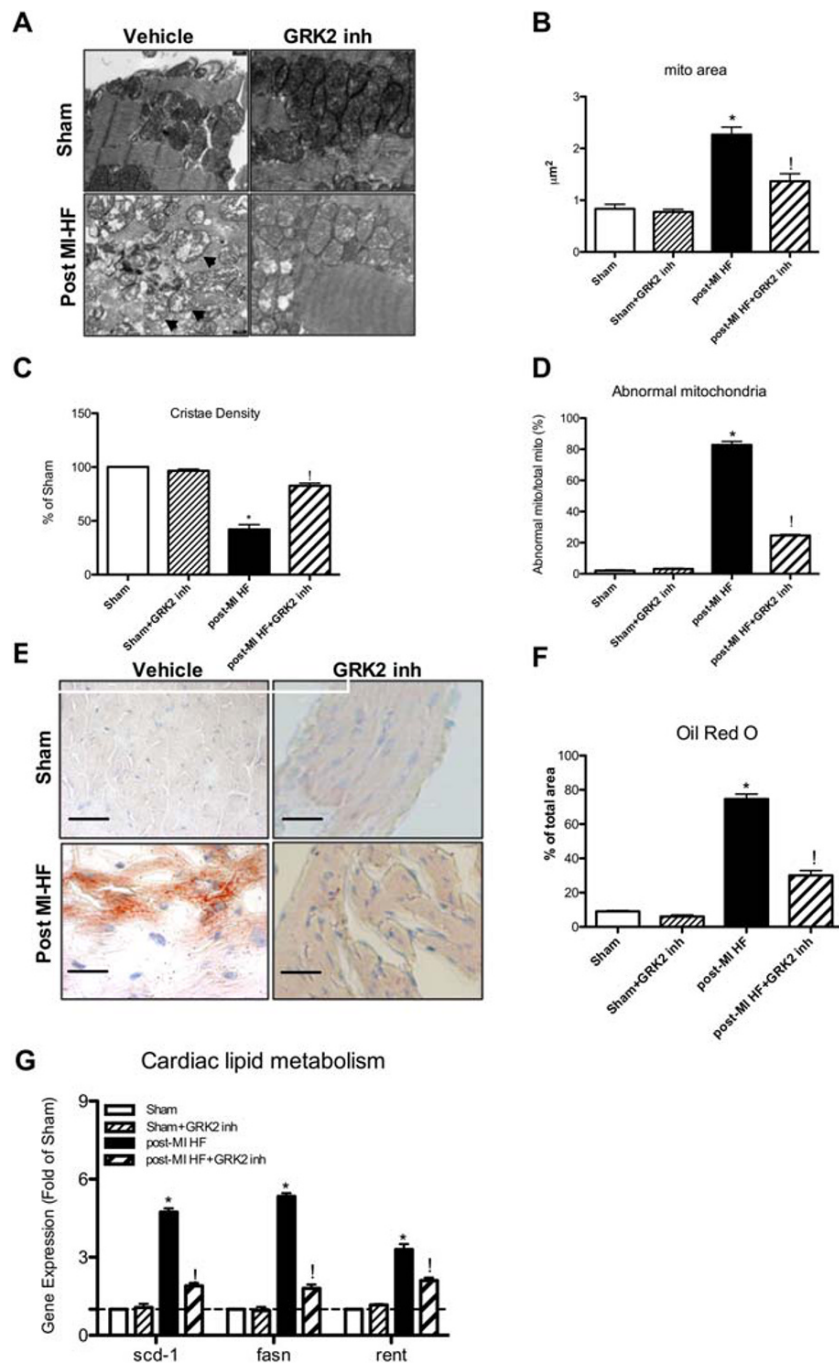


Figure 4 Mitochondrial alteration and cardiac steatosis in mice with HF. (A–D) Representative transmission electron micrographs showing abnormalities in mitochondrial ultrastructure evident in post-MI HF samples. Images show the disrupted mitochondrial structure with numerous breaks and loss of cristae structure and matrix in failing myocardium (pointed by arrows). The mitochondrial structure appears recovered by the GRK2 inhibitor in post-MI HF. Mitochondrial morphometric analyses (scale bar = 1 μm) obtained quantification of mitochondrial abnormalities with evaluation of (B) mitochondrial area, (C) percentage of abnormal mitochondria, (D) cristae density (* vs. sham, $P < 0.05$; † vs. post-MI HF, $P < 0.05$; ** vs. sham, $P < 0.05$). Quantification was performed by three blinded investigators (D. S., A. F., and C. D. G.). (E, F) Representative images (magnification 9200, scale bar = 15 μm) and quantification of Oil Red O staining showing cardiac lipid overload in post-MI HF samples (* vs. sham, $P < 0.05$) with the significant reduction after treatment with C7 inhibitor († vs. post-MI HF, $P < 0.05$). Quantification was performed by three blinded investigators (D. S., A. F., and C. D. G.). (G) Gene expression analysis by RT-PCR ($n = 4$) detects increased expression of lipid metabolism genes in hearts from post-MI HF group (* vs. sham, $P < 0.05$). GRK2 inhibitor (2 mg/kg/day) significantly reduces genes expression levels in failing hearts († vs. post-MI HF, $P < 0.05$). Data are expressed as relative gene expression (vs. sham).



GRK2 inhibition corrects aberrant mitochondria, cardiac lipid accumulation, defective mitogenesis, and ATP production during heart failure

Defective cardiac metabolism and mitochondrial dysfunction, with consequently reduced energy reserve, are hallmarks of HF^{7,27,28}.

The physiological ultrastructural localization of cardiac fibres and mitochondria consisting in sarcomeres alternating with a row of intermyofibrillar mitochondria is disarranged in post-MI HF hearts (Figure 4DA–4). Also, mitochondrial abnormalities such as swelling and loss of mitochondrial cristae and matrix are observed (Figure 4A, arrows). Increased lipid accumulation is a feature in our model of post-MI HF (Figure 4E and 4F), as expected.²⁷ Accordingly, we report the up-regulation of the critical cardiac lipid metabolism genes fatty acid synthase (*fasn*), stearoyl-Coenzyme A desaturase 1 (*scd1*), and Resistin (*rent*) (Figure 4G). Additional genes promoting mitochondrial biogenesis and adaptation to stress, like PGC1 α , and oxidative capacity such as the electron transport proteins (ETC) are deeply compromised in post-MI HF (Figure 5CA–5), leading to a significant reduction of cardiac ATP content (Figure 5D).

C7 significantly recovers mitochondrial morphology and association to cardiac fibres (Figure 4DA–4), unloads cardiac fibres from lipid accumulation, and normalizes metabolic gene profile (Figure 4GE–4). Moreover, it recovers the expression of mitochondrial biogenesis, ETC related genes, and ATP production in post-MI HF (Figure 5DA–5).

Because we measured a reduction in ATP content and an increase in disarranged mitochondrial mass, we measured mitochondrial respiration. Indeed, electron transport and ATP synthesis are tightly coupled, although a fraction of the energy generated by electron transport is usually uncoupled from ATP synthesis even in healthy cells,²⁹ and this might be increased in HF. Mitochondrial state 3 respiration rates, evaluated using succinate or pyruvate/malate as substrates, are significantly decreased in post-MI HF animals when compared with control mice (Figure 5E and 5F). GRK2 inhibitor peptide significantly recovers state 3 respiration rates in post-MI HF mice, while no effect is observed in the control group treated with C7. Similarly, oligomycin measured state 4 respiration and maximal FCCP-stimulated respiration were reduced in post-MI HF group compared with sham and significantly recovered after the treatment with GRK2 inhibitor peptide (Supporting Information, Figure S1E). No effects on mitochondrial function was observed in the control group treated with GRK2 inhibitor peptide. As a consequence, cardiac mitochondrial coupling efficiency, assessed as the ratio of the two measures, is unchanged in the different groups (data not shown). Therefore, the loss in energetic efficiency appears to be due to a global reduction in mitochondrial respiratory chain quantity, rather than to an increased mitochondrial uncoupling. GRK2 inhibition restores this quantitative impairment.

Effects of GRK2 inhibition on β AR signalling

Myocardial infarction heart failure hearts show impaired β AR signalling that is recovered by the C7 (Figure 6A). Indeed, as described in Figure 6B, both basal and ISO-stimulated cAMP production is restored in C7 compared with sham-treated post-MI HF mice.

Defective β AR signalling is tightly bound to GRK2 activity, which is known to be up-regulated in HF.¹⁰ We confirmed these results in whole hearts from post-MI HF mice where GRK2 level (Supporting Information, Figure S2B and S2C) and activity significantly increases (Figure 6C and 6D). GRK2 inhibitor peptide potently reduces kinase activity in HF as measured by rhodopsin assay (Figure 6C and 6D). It is known that GRK2 inhibition leads to a compensatory increase of other GRKs such as GRK5.³⁰ Interestingly, chronic treatment with C7 in sham increases GRK2 level but without enhancing the overall kinase activity.

Improvement of the systemic haemodynamic in post myocardial infarction heart failure mice induced by GRK2 inhibition

In HF, as shown in Figure 7A and 7B, urine volume is reduced along with decreased urine Na/K ratio. Treatment with C7 restores Na/K ratio and increases urine volume in HF mice. The ameliorated haemodynamic (Figure 7C) and increased Na excretion leads to reduced interstitial oedema as indicated by the reduced lung weight/body weight ratio in this group (Figure 7D). Finally, C7 fosters the reduction of BNP and ANF mRNA cardiac levels and restores SERCA2a mRNA level (Figure 7E). C7 does not increase urine volume and affect blood pressure in sham animal (Figure 7CA–7). This last result underlines the difference between acute and chronic administration of C7.

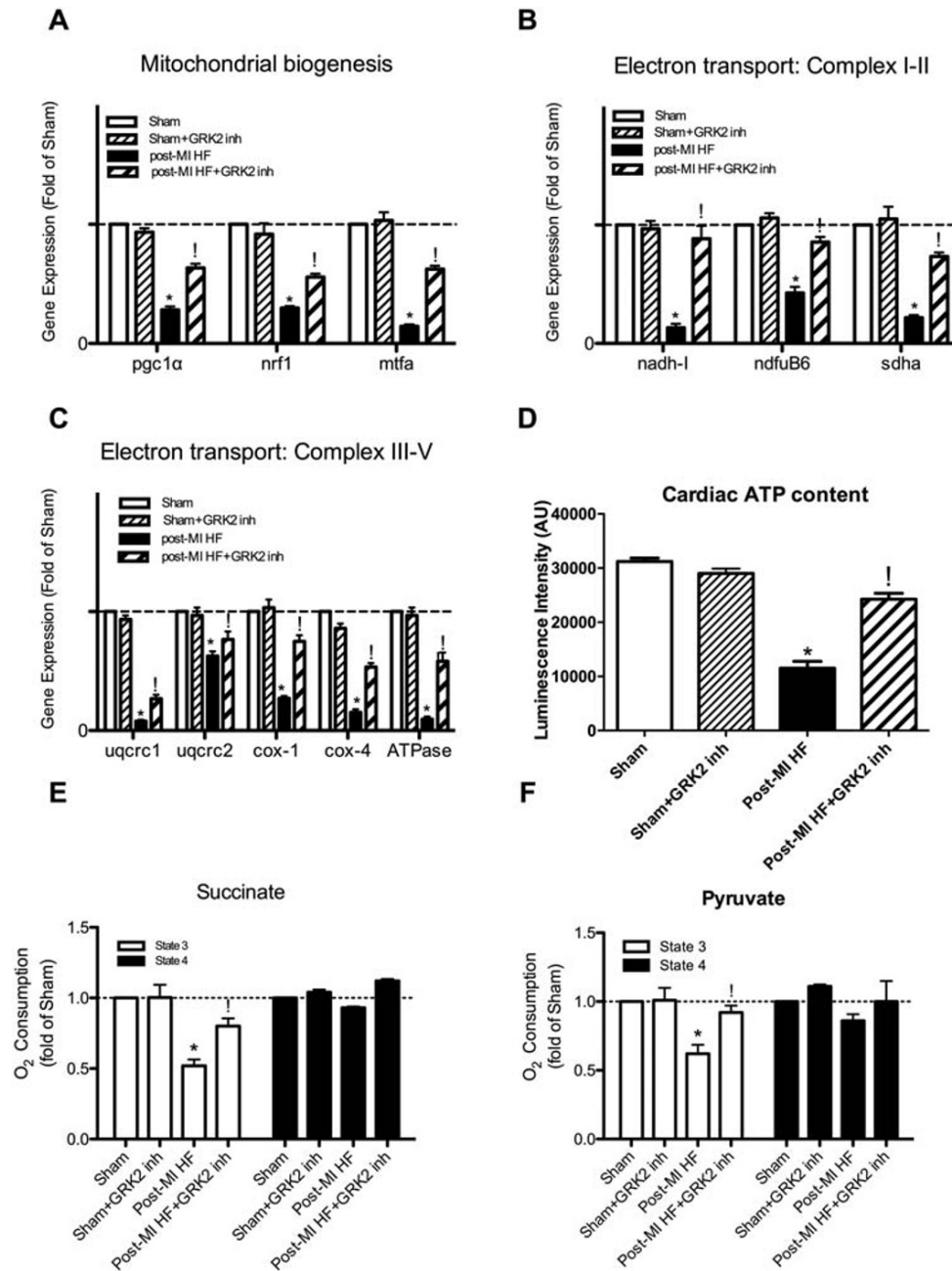
Discussion

Our study demonstrates that a novel strategy for GRK2 inhibition based on HJ loop competition retains the known therapeutic effects in experimental HF. In particular, we demonstrate the amelioration of cardiac remodelling, contractility, and haemodynamics and extend the finding to metabolic and energetic phenotypes in failing mice.

The first purpose of our study was to finally demonstrate that C7 acts through means of GRK2 inhibition. The lack of effect of C7 in cardiac myocytes that do not express GRK2 due to selective genetic deletion clarifies this issue and allows us to consider C7 a selective GRK2 inhibitor.

Previous works, employing different strategies of GRK2 inhibition, demonstrated that the reducing the activity of this

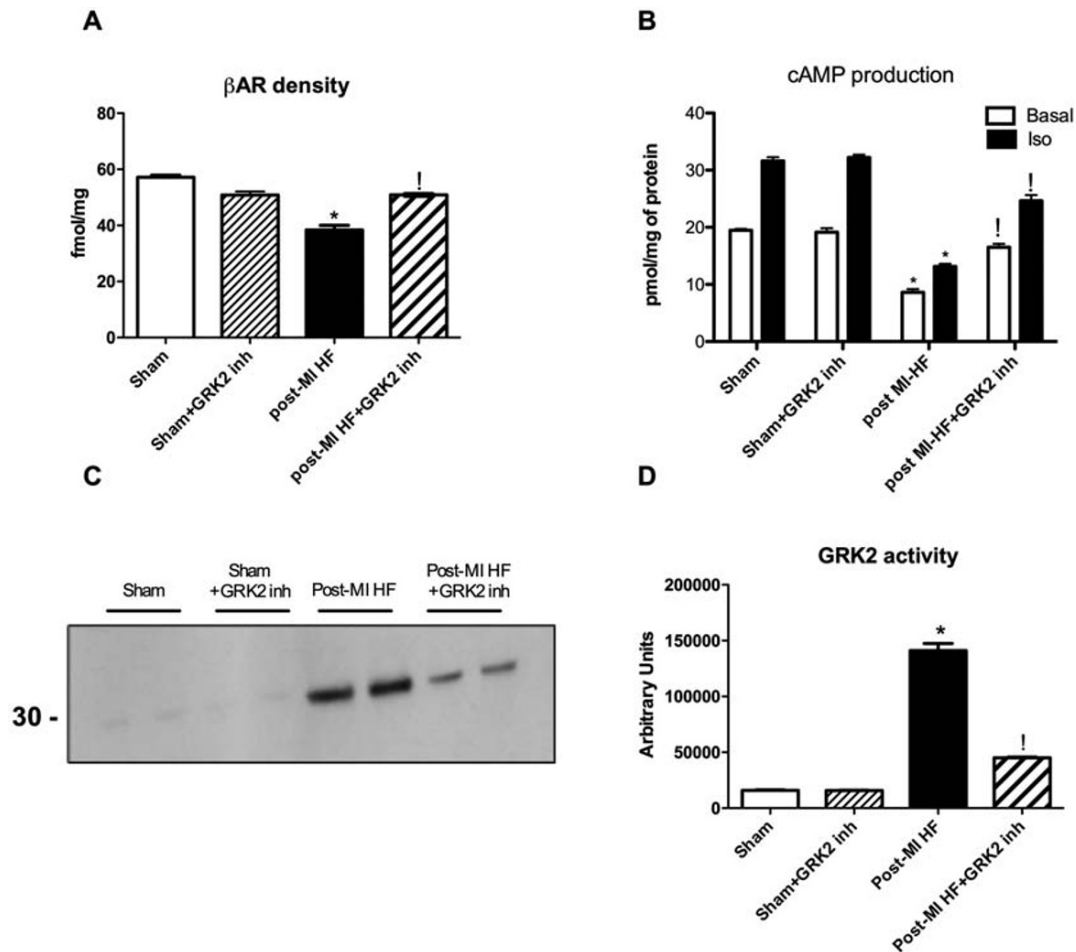
Figure 5 Cardiac metabolic and mitochondrial alterations in HF. (A–D) Regulators of mitogenesis and electron transport related genes measured by RT-PCR. Defective expression of PGC1 α , NRF1, MTFA, ETC complex can be observed in post-MI HF group (* vs. sham, $P < 0.05$). GRK2 inhibitor (2 mg/kg/day) significantly improves genes expression levels in failing hearts (! vs. post-MI HF, $P < 0.05$). Data are expressed as relative gene expression (vs. sham). (E) ATP production measured by luminescence assay. ATP content significantly reduced in post-MI HF (* vs. sham, $P < 0.05$). GRK2 inhibitor treatment improves ATP levels during HF (! vs. post-MI HF, $P < 0.05$). (E, F) Mitochondrial respiration. Mitochondrial state 3 respiration rates evaluated using succinate or pyruvate as substrates are significantly decreased in post-MI HF versus sham (*, $P < 0.05$). GRK2 inhibitor peptide significantly recovers state 3 respiration rates in post-MI HF animals (! vs. post-MI HF, $P < 0.05$). ETC, electron transport chain; MTFA, mitochondrial transcription factor A; NRF1, nuclear respiratory factor; PGC1 α , peroxisome proliferator-activated receptor gamma coactivator 1-alpha; RT-PCR, real-time-polymerase chain reaction; other abbreviations as in previous figures.



kinase is possible to restore myocardial function at biochemical and contractile level.³¹ In the current work, we confirmed these results showing cardiac reverse remodelling, direct

restoration of the β adrenergic signalling and, probably indirectly, of SERCA2a expression due to the global improvement of the cardiac functions.

Figure 6 Effects of GRK2 inhibition on β AR signalling. (A) β AR density measured by radioligand binding assay on isolated plasma membrane from heart samples. Samples from post-MI HF display a decreased β AR density (* vs. sham, $P < 0.05$) but restored by GRK2 inhibitor treatment at 2 mg/kg/day (! vs. post-MI HF). (B) cAMP content and production after iso stimulation (0.1 μ M) evaluated on heart samples. Post-MI HF has a decreased cAMP production at both baseline, and iso stimulated conditions (* vs. sham, $P < 0.05$) but recovered in the presence of GRK2 inhibitor treatment (! vs. post-MI HF, $P < 0.05$). (C, D) Kinase activity evaluated by Rhodopsin phosphorylation. Representative autoradiography image shows significantly increased rhodopsin phosphorylation in heart sample from post-MI HF group (* vs. sham, $P < 0.05$) with significant reduction when C7 is present (! vs. post-MI HF, $P < 0.05$).



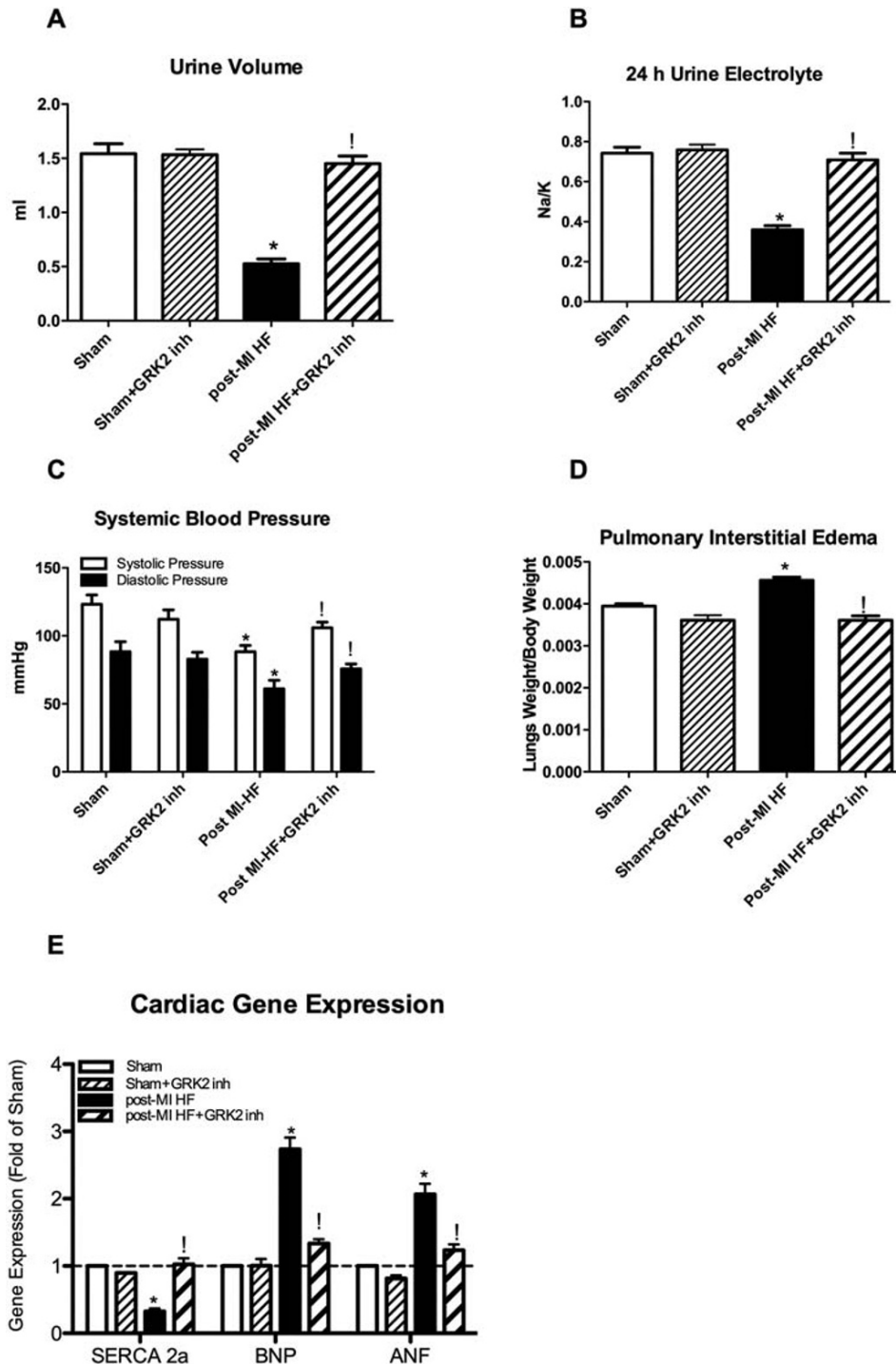
However, the mechanisms of HF are manifold, and mitochondrial dysfunction appears to be an early mechanism that precedes systolic dysfunction³² and increased GRK2 levels participate in this setup.^{7,33} We show, for the first time, that GRK2 inhibition ameliorates mitochondrial biogenesis and cardiac ATP content. Indeed, our results demonstrate that mitogenesis and ATP production are strongly compromised in post-MI HF mice and that GRK2 inhibitor peptide partially recovers these functions.

Previous studies on GRK2 inhibition in HF have only focused on cardiac contractility and β AR signalling, evidencing the ability to protect β ARs to the same extent and even potentiating the effects of beta-blockers,¹⁵ but no effects on cardiac mitochondrial and energetic have been demonstrated so far. Now, we demonstrate that GRK2 inhibition works in a comprehensive manner in HF. Indeed, GRK2 is a critical

modulator of metabolism,³⁴ and its up-regulation in HF induces cardiac insulin resistance⁷ and reduces free fatty acid utilization,³³ increases catecholamine secretion from the adrenal gland^{35,36} and aldosterone level through β Arrestin1.³⁷ Therefore, GRK2 pharmacological inhibition might have positive effects on cardiac metabolism, as already observed in diabetes¹⁹ and hypertension,²⁰ as well as systemic effects on other organs. Our results demonstrate that it is possible to pharmacologically target the metabolic alterations induced by GRK2 up-regulation. Furthermore, we extend this notion to the observation that mitochondria aberrations can be corrected by inhibition of GRK2. Therefore, in adjunction to the expected effects on β AR signalling, GRK2 inhibition exerts also beneficial effects in mitochondria.

GRK2 is a ubiquitous molecule and can increase in chronic HF in several organs beyond the heart, which renders difficult

Figure 7 Improved systemic haemodynamic in mice with HF. (A, B) 24 h urine volume and Na/K ratio. Urine volume collected in 24 h is significantly reduced in animals with HF, with reduced Na/K ratio in the same sample (* vs. sham, $P < 0.05$). GRK2 inhibitor treatment (2 mg/kg/day) increases both volume and Na/K ratio in urine collected after 24 h ([†] vs. post-MI HF). (C) Interstitial pulmonary oedema is measured by lung to body weight ratio. HF is associated with a significant increase in lung weight ([†] vs. sham, $P < 0.05$;) but reduced by the GRK2 inhibitor at 2 mg/kg/day ([†] vs. post-MI HF, $P < 0.05$). (D) SP measured in conscious animals by the tail cuff. SP is reduced in post-MI HF group in both diastolic and systolic values (* vs. sham, $P < 0.05$) but recovered with treatment ([†] vs. post-MI HF, $P < 0.05$). (E) SERCA2a, BNP, and ANF mRNA level measured by RT-PCR on heart samples. HF is associated with decreased SERCA2a and increased BNP, ANF mRNA level (* vs. sham, $P < 0.05$). The expression level of these is normalized by treatment with GRK2 inhibitor ([†] vs. post-MI HF, $P < 0.05$). Significant modifications of SERCA2a and BNP level are also observed in sham animals undergone treatment (** vs. sham, $P < 0.05$). Data are expressed as relative gene expression (vs. sham). ANF, atrial natriuretic factor; BNP, brain natriuretic peptide; Na, sodium; K, potassium; SERCA2a, sarco/endoplasmic reticulum Ca^{2+} -ATPase; SP, systemic blood pressure.



to discern which cellular type is mostly evoked. Although no specifically designed, our study allows to compare some systemic effects of the chronic administration of GRK2 inhibitor peptide versus vehicle in sham animals. Collectively, our treatment appears specifically targeted for cardiac GRK2, where its inhibition improves cardiovascular function, haemodynamic state, and renal perfusion with increased diuresis.

Our data allow a distinction of the effects of GRK2 inhibition between acute and chronic administration, as well as between healthy and failing phenotypes. Acute administration of C7 leads to a rapid increase of cardiac rate and contractility, showing positive inotropism properties. Chronic infusion (2 mg/kg) in healthy mice, though, increases the levels of GRK2, suggesting that a physiological minimal activity of the kinase is indeed needed. Interestingly, the same dose chronically administered in the failing mouse produces normalization of exaggerated GRK2 levels and a beneficial effect on signalling. Collectively, these results support the very critical role of GRK2 to provide a shift between healthy and diseased phenotypes in the heart. Acting on this switch has the potentiality to be a pharmacological target.

Our data propose that chronic inhibition of GRK2 in the condition characterized by excessive GRK2 level and activity have protective effects on the mitochondria. Nevertheless, in different setup, like in the presence of acute distress, preserved GRK2 activity might be necessary to maintain normal mitochondrial health, through the regulation of mitochondrial dynamics.⁸

The impact of a GRK2 inhibitor on the human therapy for HF at the moment cannot be predicted. Some features of GRK2 inhibition make this therapeutic target unique. First of all, acutely, C7 in non-failing cardiomyocytes is a direct positive inotrope. This is a peculiar feature in comparison with RAS inhibitors and to beta-blockers, which, opposite, inhibit contractility. Second, chronic infusion of GRK2 inhibitors result in metabolic and biochemical changes that anticipate the positive effect on cardiac function. Positive inotropism and favourable metabolism are two mechanisms that could well complement with adrenergic beta-blocker. Similarly, all the mechanisms of the RAS land on the amelioration of the angiotensin receptor signalling, a feature that could be easily anticipated by the inhibition of GRK2, which act as regulator also to the AT receptors. Furthermore, GRK2 inhibition could be an appropriate drug for those patients that cannot be treated with RAS inhibitors or beta-blockers.

In conclusion, we provide the evidence that the HJ loop targeting of GRK2 through C7 is useful in an animal model of HF, and it represents a prototype of first-in-class drugs specifically able to modulate GRK2 activity. Moreover, our study is the first to demonstrate that a pharmacological strategy of GRK2 inhibition is active also on cardiac metabolism and substrate utilization, which are early affected during HF. Also, it brings further confirmation of GRK2 as a molecular target in HF.

Indeed, the ability of C7 to recover the expression of mitochondrial biogenesis, ETC related genes, ATP production, and mitochondrial function in post-MI HF hearts could represent a promising direction that may soon yield effective treatments to restore myocardial function in HF.

Finally, our study reduces the distance for the GRK2 direct inhibition towards the use in humans, by providing an alternative tool to inhibit GRK2.

Study limitations

This study focused mainly on the demonstration that C7 is effective in an experimental model of HF; however, further studies are needed to identify pharmacokinetic features. Indeed, the use of chronic constant infusion with the miniosmotic pumps does not allow any investigation of pharmacokinetics.

Given the complexity of the GRK2 interactome, it is most likely that C7 interferes also with other mechanisms of HF. Further investigation is warranted to clarify this issue.

Moreover, as a preclinical study, our compound needs to be also tested in a larger animal model of HF. Further work is also required to identify small molecules targeting the HJ loop of GRK2 with kinetic and dynamic properties to achieve easier delivery of GRK2 inhibition.

Acknowledgements

We thank Dr. A. Ninni for his technical support in measuring serum electrolytes in mice. We also thank Prof. Petronila Penela for the GRK2 fl/fl mice.

Conflict of interest

None declared.

Funding

This work was in part supported by grants from Italian Ministry of Instruction, University and Research (PRIN 2017 and PON Campania Bioscience PON03PE0006008 to G. I.), POR MOVIE from Regione Campania Rete di Biotecnologie (G. I.), University of Salerno's Funds for Basic Research (FARB to G. I. and M. C.), and Italian Society of Hypertension (SIIA to G. I.).

Conflict of interest

G. I. is a consultant for Amicus Therapeutics. All other authors declare no conflict of interest.

Supporting information

Additional supporting information may be found online in the Supporting Information section at the end of the article.

Table S1. Heart Rate and Cardiac ultrasound measurements in post MI mice. Data are presented as mean \pm SEM. Sham: Control group. Sham+GRK2 inh: Sham treated with GRK2 inh. Post-MI HF: post MI group treated with vehicle. LVDD: Left Ventricle end Diastolic diameter. EF: Ejection Fraction (* vs. Sham, $P < 0.05$; ! vs. post MI-HF, $P < 0.05$).

Fig 1. A. Representative image of Myocardial infarction evaluated by staining (Evans Blue) and Echocardiography **B.** Systemic Blood pressure measured by tail cuff. GRK2 inhibition significantly increases blood pressure at 10' and 30' with the return to baseline at 90' post injection (* $P < 0.05$ vs. vehicle). **C.** cAMP production evaluated at baseline and 30' post C7 or vehicle injection on heart samples. GRK2 inhibitor significantly increases cAMP production at 30' post injection. (* $P < 0.05$ vs. vehicle). **C.** Representative ultrasound images

of cardiac dimensions pre and at 2, 6 and 10 weeks post surgery. **D-E:** Masson's trichrome staining ($n = 4$ per group) on left ventricle cross section shows reduction of the infarct size in post-MI HF treated with C7 (* $P < 0.05$, vs vehicle). Quantification was performed by three blinded investigators (DS, AF, CDG).

Fig 2. A. Oligomycin and maximal FCCP-stimulated respiration are significantly reduced in in post MI-HF group versus Sham (* vs. Sham, $P < 0.05$), and recovered after the treatment with GRK2 inhibitor peptide (! vs. post-MI, $P < 0.05$). **B-C:** Western blots representative images (left panels) and densitometric analysis (right panels) of GRK2 levels in the whole lysate obtained from heart samples ($n = 3$ per group). GRK2 is increased during HF (* vs Sham, $P < 0.05$) with significant reduction of the GRK2 level was produced by treatment during HF (! vs post MI-HF, ns). Sham animal treated with GRK2 inhibitor showed increased level of the kinase (** vs Sham, $P < 0.05$).

References

1. Ingwall JS. Energy metabolism in heart failure and remodelling. *Cardiovasc Res* 2009; **81**: 412–419.
2. Akhmedov AT, Rybin V, Marin-Garcia J. Mitochondrial oxidative metabolism and uncoupling proteins in the failing heart. *Heart Fail Rev* 2015; **20**: 227–249.
3. Mudd JO, Kass DA. Tackling heart failure in the twenty-first century. *Nature* 2008; **451**: 919–928.
4. Piacentino V 3rd, Weber CR, Chen X, Weisser-Thomas J, Margulies KB, Bers DM, Houser SR. Cellular basis of abnormal calcium transients of failing human ventricular myocytes. *Circ Res* 2003; **92**: 651–658.
5. Katz MG, Fargnoli AS, Swain JD, Tomasulo CE, Ciccarelli M, Huang ZM, Rabinowitz JE, Bridges CR. AAV6- β ARKct gene delivery mediated by molecular cardiac surgery with recirculating delivery (MCARD) in sheep results in robust gene expression and increased adrenergic reserve. *J Thorac Cardiovasc Surg* 2012; **143**: 720–726 e723.
6. Koch WJ, Rockman HA, Samama P, Hamilton RA, Bond RA, Milano CA, Lefkowitz RJ. Cardiac function in mice overexpressing the beta-adrenergic receptor kinase or a beta ARK inhibitor. *Science* 1995; **268**: 1350–1353.
7. Ciccarelli M, Chuprun JK, Rengo G, Gao E, Wei Z, Peroutka RJ, Gold JI, Gumpert A, Chen M, Otis NJ, Dorn GW 2nd, Trimarco B, Iaccarino G, Koch WJ. G protein-coupled receptor kinase 2 activity impairs cardiac glucose uptake and promotes insulin resistance after myocardial ischemia. *Circulation* 2011; **123**: 1953–1962.
8. Franco A, Sorriento D, Gambardella J, Pacelli R, Prevet N, Procaccini C, Matarese G, Trimarco B, Iaccarino G, Ciccarelli M. GRK2 moderates the acute mitochondrial damage to ionizing radiation exposure by promoting mitochondrial fission/fusion. *Cell Death Dis* 2018; **4**: 25.
9. Chen M, Sato PY, Chuprun JK, Peroutka RJ, Otis NJ, Ibeti J, Pan S, Sheu SS, Gao E, Koch WJ. Prodeath signaling of G protein-coupled receptor kinase 2 in cardiac myocytes after ischemic stress occurs via extracellular signal-regulated kinase-dependent heat shock protein 90-mediated mitochondrial targeting. *Circ Res* 2013; **112**: 1121–1134.
10. Iaccarino G, Koch WJ. Therapeutic potential of G-protein coupled receptor kinases in the heart. *Expert Opin Investig Drugs* 1999; **8**: 545–554.
11. Rengo G, Lympopoulos A, Zincarelli C, Donniacuo M, Soltys S, Rabinowitz JE, Koch WJ. Myocardial adeno-associated virus serotype 6- β ARKct gene therapy improves cardiac function and normalizes the neurohormonal axis in chronic heart failure. *Circulation* 2009; **119**: 89–98.
12. Homan KT, Tesmer JJ. Molecular basis for small molecule inhibition of G protein-coupled receptor kinases. *ACS Chem Biol* 2015; **10**: 246–256.
13. Homan KT, Larimore KM, Elkins JM, Szklarz M, Knapp S, Tesmer JJ. Identification and structure-function analysis of subfamily selective G protein-coupled receptor kinase inhibitors. *ACS Chem Biol* 2015; **10**: 310–319.
14. Homan KT, Wu E, Wilson MW, Singh P, Larsen SD, Tesmer JJ. Structural and functional analysis of G protein-coupled receptor kinase inhibition by paroxetine and a rationally designed analog. *Mol Pharmacol* 2014; **85**: 237–248.
15. Schumacher SM, Gao E, Zhu W, Chen X, Chuprun JK, Feldman AM, Tesmer JJ, Koch WJ. Paroxetine-mediated GRK2 inhibition reverses cardiac dysfunction and remodeling after myocardial infarction. *Sci Transl Med* 2015; **7**: 277ra31.
16. Lowe JD, Sanderson HS, Cooke AE, Ostovar M, Tsisanova E, Withey SL, Chavkin C, Husbands SM, Kelly E, Henderson G, Bailey CP. Role of G protein-coupled receptor kinases 2 and 3 in mu-opioid receptor desensitization and internalization. *Mol Pharmacol* 2015; **88**: 347–356.
17. Carotenuto A, Cipolletta E, Gomez-Monterrey I, Sala M, Vernieri E, Limatola A, Bertamino A, Musella S, Sorriento D, Grieco P, Trimarco B, Novellino E, Iaccarino G, Campiglia P. Design, synthesis and efficacy of novel G protein-coupled receptor kinase 2 inhibitors. *Eur J Med Chem* 2013; **69**: 384–392.
18. Gomez-Monterrey I, Carotenuto A, Cipolletta E, Sala M, Vernieri E, Limatola A, Bertamino A, Musella S, Grieco P, Trimarco B, Novellino E, Iaccarino G, Campiglia P. SAR study and conformational analysis of a series of novel peptide G protein-coupled receptor kinase

- 2 inhibitors. *Biopolymers* 2014; **101**: 121–128.
19. Cipolletta E, Gambardella J, Fiordelisi A, Del Giudice C, Di Vaia E, Ciccarelli M, Sala M, Campiglia P, Coscioni E, Trimarco B, Sorriento D, Iaccarino G. Antidiabetic and cardioprotective effects of pharmacological inhibition of GRK2 in db/db mice. *Int J Mol Sci* 2019; **20**.
 20. Cipolletta E, Campanile A, Santulli G, Sanzari E, Leosco D, Campiglia P, Trimarco B, Iaccarino G. The G protein coupled receptor kinase 2 plays an essential role in beta-adrenergic receptor-induced insulin resistance. *Cardiovasc Res* 2009; **84**: 407–415.
 21. Matkovich SJ, Diwan A, Klanke JL, Hammer DJ, Marreez Y, Odley AM, Brunskill EW, Koch WJ, Schwartz RJ, Dorn GW 2nd. Cardiac-specific ablation of G-protein receptor kinase 2 redefines its roles in heart development and beta-adrenergic signaling. *Circ Res* 2006; **99**: 996–1003.
 22. Kilkenny C, Browne W, Cuthill IC, Emerson M, Altman DG, Group NCRGW. Animal research: reporting in vivo experiments: the ARRIVE guidelines. *Br J Pharmacol* 2010; **160**: 1577–1579.
 23. McGrath JC, Drummond GB, McLachlan EM, Kilkenny C, Wainwright CL. Guidelines for reporting experiments involving animals: the ARRIVE guidelines. *Br J Pharmacol* 2010; **160**: 1573–1576.
 24. Pleger ST, Most P, Boucher M, Soltys S, Chuprun JK, Pleger W, Gao E, Dasgupta A, Rengo G, Remppis A, Katus HA, Eckhart AD, Rabinowitz JE, Koch WJ. Stable myocardial-specific AAV6-S100A1 gene therapy results in chronic functional heart failure rescue. *Circulation* 2007; **115**: 2506–2515.
 25. Santulli G, Cipolletta E, Sorriento D, Del Giudice C, Anastasio A, Monaco S, Maione AS, Condorelli G, Puca A, Trimarco B, Illario M, Iaccarino G. CaMK4 gene deletion induces hypertension. *J Am Heart Assoc* 2012; **1**: e001081.
 26. Gao E, Lei YH, Shang X, Huang ZM, Zuo L, Boucher M, Fan Q, Chuprun JK, Ma XL, Koch WJ. A novel and efficient model of coronary artery ligation and myocardial infarction in the mouse. *Circ Res* 2010; **107**: 1445–1453.
 27. Abdalla S, Fu X, Elzahwy SS, Klaetschke K, Streichert T, Quitterer U. Up-regulation of the cardiac lipid metabolism at the onset of heart failure. *Cardiovasc Hematol Agents Med Chem* 2011; **9**: 190–206.
 28. Zhang L, Jaswal JS, Ussher JR, Sankaralingam S, Wagg C, Zaugg M, Lopaschuk GD. Cardiac insulin-resistance and decreased mitochondrial energy production precede the development of systolic heart failure after pressure-overload hypertrophy. *Circ Heart Fail* 2013; **6**: 1039–1048.
 29. Stucki JW. The optimal efficiency and the economic degrees of coupling of oxidative phosphorylation. *Eur J Biochem* 1980; **109**: 269–283.
 30. Salazar NC, Vallejos X, Siryk A, Rengo G, Cannavo A, Liccardo D, De Lucia C, Gao E, Leosco D, Koch WJ, Lympopoulos A. GRK2 blockade with β ARKct is essential for cardiac β 2-adrenergic receptor signaling towards increased contractility. *Cell Commun Signal* 2013; **11**: 64.
 31. Sorriento D, Ciccarelli M, Cipolletta E, Trimarco B, Iaccarino G. "Freeze, don't move": how to arrest a suspect in heart failure - a review on available GRK2 inhibitors. *Front Cardiovasc Med* 2016; **3**: 48.
 32. Bayeva M, Gheorghide M, Ardehali H. Mitochondria as a therapeutic target in heart failure. *J Am Coll Cardiol* 2013; **61**: 599–610.
 33. Pflieger J, Gross P, Johnson J, Carter RL, Gao E, Tilley DG, Houser SR, Koch WJ. G protein-coupled receptor kinase 2 contributes to impaired fatty acid metabolism in the failing heart. *J Mol Cell Cardiol* 2018; **123**: 108–117.
 34. Sorriento D, Ciccarelli M, Santulli G, Illario M, Trimarco B, Iaccarino G. Trafficking GRK2: cellular and metabolic consequences of GRK2 subcellular localization. *Transl Med UniSa* 2014; **10**: 3–7.
 35. Lympopoulos A, Rengo G, Funakoshi H, Eckhart AD, Koch WJ. Adrenal GRK2 upregulation mediates sympathetic overdrive in heart failure. *Nat Med* 2007; **13**: 315–323.
 36. Lympopoulos A, Rengo G, Gao E, Ebert SN, Dorn GW 2nd, Koch WJ. Reduction of sympathetic activity via adrenal-targeted GRK2 gene deletion attenuates heart failure progression and improves cardiac function after myocardial infarction. *J Biol Chem* 2010; **285**: 16378–16386.
 37. Lympopoulos A, Rengo G, Zicarelli C, Kim J, Soltys S, Koch WJ. An adrenal beta-arrestin 1-mediated signaling pathway underlies angiotensin II-induced aldosterone production in vitro and in vivo. *Proc Natl Acad Sci U S A* 2009; **106**: 5825–5830.